6.24

DO MULTIPLE PEAKS IN THE RADON TRANSFORM OF WESTWARD PROPAGATING SEA SURFACE HEIGHT ANOMALIES CORRESPOND TO HIGHER ORDER ROSSBY WAVE BAROCLINIC MODES?

A. Maharaj[1], P. Cipollini[2]and N. Holbrook[3]
[1,3]Macquarie University, Sydney, Australia
[2]Southampton Oceanography Center, Southampton, United Kingdom

1 Introduction

Long wavelength baroclinic oceanic Rossby waves play a significant role in ocean dynamics. They maintain and influence the strong western boundary currents, are the main oceanic response to changes in atmospheric forcing and are an indicator of the length of time that anomalous conditions persist (Gill 1982) . However, due to their small sea surface signature ($<$0.1 m) and slow propagation speeds ($<$0.1 m/s), detection of these waves was nearly impossible prior to the advent of satellite altimetry. With more than a decade of altimeter data from the TOPEX/Poseidon (T/P) satellite and prior missions, it is now possible to examine Rossby waves at the basin wide or global scale with centimeter accuracy (see Fu and Chelton (2001) for a review). These observations are a particularly valuable resource for areas where *in situ* observations are scarce, such as in the South Pacific Ocean.

Due to their westward propagation, the surface signature of Rossby waves is clearly visible in longitude-time plots (also known as Hovmöller diagrams) of sea surface height anomalies (SSHA) and to some extent in sea surface temperature (SST) and ocean colour data (Cipollini et al., 1997; Hill et al., 2000). However, not all the valuable information that the data holds is readily apparent in the time domain so signal processing techniques are often utilised to further examine the observations. Two common signal processing techniques used in the detection of observed baroclinic Rossby waves from satellite data are the 2 dimensional Radon (2D-RT) and Fourier (2D-FT) Transforms. The 2D-RT provides an objective estimate of the orientation of lines in Hovmöller plots (for example, of the characteristic westward propagating ridges and troughs of SSHA that indicate Rossby wave propagation) in order to objectively calculate the speed of the dominant signal in the plot. The 2D-FT reveals the spectral components of the data so that the signal in the data can be examined in the frequency domain.

Previous literature has suggested that multiple peaks in sea surface height (SSH) and sea surface temperature (SST) spectra as detected by the 2D-RT and 2D-FT may be the surface signature of higher order baroclinic Rossby modes in the ocean (e.g., Cipollini et al. 1997; Subrahmanyam et al. 2001). Multiple peaks in the Radon Transform analysis indicate anomalies traveling at varying speeds while the Fourier Transform can detect the spectral components of multiple propagating signals.

However previous studies only examine this hypothesis at specific locations in an ocean basin. This study examines the presence of multiple peaks from 2 dimensional Fourier and Radon Transform analysis for the entire South Pacific basin from 10 years of sea level anomalies determined from ERS (European Remote Sensing satellite) and T/P altimeter observations and attempts to determine whether their speeds resemble those of higher order baroclinic Rossby wave modes.

2 Data

Maps of Sea Level Anomaly (MSLA) are provided by the Developing Use of Altimetry for Climate Studies (DUACS) which is the Collecte Localisation Satellites (CLS) near real time multi-mission altimeter data processing system. MSLA are obtained from a complete reprocessing of T/P and ERS-1/2 data. There is one map every 7 days for a period of almost 10 years (14 October 1992 to 7 August 2002). T/P maps are available for that entire time period, but there are no T/P+ERS combined maps between January 1994 and March 1995 when ERS-1 was in geodetic phase. From June 1996 to February 2002, ERS-2 data are used. Details of the data processing and mapping method can be found in Le Traon and Ogor (1998) and Le Traon et al. (1998) . The reader is also referred to the DUACS handbook (www.jason.oceanobs.com/documents/donnees/duacs/handbook_duacs_uk.pdf) for further details.

Maps are provided on a MERCATOR $\frac{1}{3}^{\circ}$ grid, i.e., at $\frac{1}{3}^{\circ}$ in longitude with latitude adjusted accordingly. Resolution of kilometers in latitude and longitude are thus identical and vary with the cosine of latitude (e.g., from 37 km at the equator to 18.5 km at 60°N/S). Units are in centimeters. This study focuses on the South Pacific Ocean from 10°S to 50°S.

3 Method

3.1 Data treatment

Longitude-time series were extracted from the MSLA dataset for every 1° of latitude with a 20° longitude running window from 10°S to 50°S. Windows or data blocks with land were filled with a Gaussian interpolation scheme if the gap width was less than 10% of the window. Otherwise, the land was left in. Spikes and outliers in the dataset

[1]*Corresponding author address:* Angela Maharaj, Department of Physical Geography, Macquarie University, NSW 2109, Australia; email: amaharaj@penman.es.mq.edu.au

were identified as more than three standard deviations away from the mean and removed. These data were then Gaussian interpolated. The two dimensional Gaussian interpolation scheme places greater emphasis on space than in time because it is expected that the values will be more closely related in space. The full-width half maximum (FWHM) and search radius were set to $\frac{2}{3}^{\circ}$ and 1° in space and 1.4 days and 7 days in time.

Each window or data block is zero padded and passed through what we refer to as the 'westward-only' filter (Cipollini et al. 2001; Cipollini et al. 2004). This filter removes stationary and eastward propagating signals (the second and fourth quadrants in wavenumber frequency space) leaving only westward propagating signals (the first and third quadrants). This effectively also removes the annual standing signal. Additionally, a few more spectral bins around the annual peak are forced to zero to effectively remove any stationary quasi-annual signal. The Radon and Fourier Transform analysis were then carried out. Both methods are detailed in the following subsections.

Basin wide median speeds calculated from both analysis for every latitude are compared against linear theory estimates for the first baroclinic mode and against modified theory estimates for up to the fourth baroclinic mode. The latter estimates are calculated by Killworth and Blundell (2003a,b) for a fully perturbed and modified ocean bottom with 1° resolution bathymetry.

3.2 2D-Radon Transform

The two-dimensional Radon Transform (2D-RT) can be utilized to determine an objective estimate of the orientation of lines in a Hovmöller plot in order to objectively calculate the speed of the dominant signal in the image. The 2D-RT $p(x', \phi)$ at a given angle, ϕ, is a projection of the image intensity along a radial line oriented along a direction normal to ϕ (Deans 1983, Challenor et al., 2001)

$$p(x', \phi) = \int_{y'} f(x, y) \Big|_{\substack{x = x' cos\phi - y' sin\phi \\ y = x' sin\phi + y' cos\phi}} dy' \quad (1)$$

Alignments of the data at an angle in longitude-time space are lines of constant speed. When ϕ is orthogonal to the direction of the alignments in the plot, the Radon energy is maximum. Computing the RT of a Hovmöller for different values of ϕ, and then its energy, allows one to find the value of ϕ for which the energy is maximum. This objectively determines the angle of the predominant energy signal in the data. The corresponding speed can then be readily calculated from ϕ from simple trigonometric considerations, being proportional to tan(ϕ) (Cipollini et al. 2004).

The 2D-RT was calculated for each longitude-time series for ϕ ranging from 0° - 90° (every 1°). Peaks were detected by examining the first and second derivatives of the standard deviation of the Radon Energy. The first derivative is smoothed with a 5 point boxcar filter before computing the second derivative. Speeds are then computed for angles that show a peak in the Radon energy by multiplying the tan of the angle with the ratio of the longitude resolution and the time resolution. The significance of each peak is tested by calculating its relative height. This is a ratio of the peak to the mean value as used and defined in Hill et al., (2000) . Distance of peak from mean value was also calculated.

3.3 2D Fourier Transform

A 2 dimensional Fast Fourier Transform (2D-FT) algorithm can be used to examine the spectral components of the data blocks. A 2D-FT allows a signal to be examined in its frequency domain which can highlight valuable information not readily apparent in the time domain (i.e in the hovmollers which show space over time). It allows the detection of the single components of the propagating signals which may correspond to different baroclinic modes (e.g., Cipollini et al. 1997; Subrahmanyam et al. 2001). The 2D-FT is an extension of the one-dimensional Fourier Transform and in practice is implemented with the Fast Fourier Transform (Brigham 1988). The 2D-FT is given by

$$S(f_x, f_y) = \Delta x, \Delta y \sum_{m=1}^{M} \sum_{n=1}^{N} s(m\Delta x, n\Delta y) e^{-j\,2\pi (f_x \Delta x + f_y \Delta y)} \quad (2)$$

for a Hovmöller, $s(m\Delta x, n\Delta y)$ of $M \times N$ pixels, where m, n are the pixel indices and $\Delta x, \Delta y$ the pixel dimensions in the x (longitude) and y (time) directions. This is computed on a discrete grid $S(p\Delta f_x, q\Delta f_y)$ where $p = 1 \ldots M$, $q = 1 \ldots N$ with frequency resolutions $\Delta f_x = 1/(M\Delta x)$ and $\Delta f_y = 1/(N\Delta y)$. S is periodic in both f_x and f_y with periods $1/\Delta x$ and $1/\Delta y$ (Cipollini et al. 2004)

The 2D-FT is performed and the power spectra is calculated by squaring the sum of the real and imaginary parts of the transform. The origin is shifted to the centre so that the zero frequency component will be in the middle of the spectrum. The spectrum is also flipped so that westward propagating features are in the left part of the spectrum. Peaks in the spectrum and their corresponding wavelength and frequencies were found. Speeds are readily calculated by dividing the frequency over the wavenumber.

4 Results

4.1 2D Radon Transform

Figure 1 shows the Rossby wave speeds calculated from the first peak in the 2D-RT analysis as well as the peak amplitude (standard deviation of the energy) and its relative height, ie., its ratio to mean peak value.

In general, there are faster speeds equatorwards and slower speeds polewards. In the mid-latitudes, speeds increase on the western side of the basin. Between 10°S and 15°S, however, some significantly slower speeds can be seen in the mid to western side. These have been shown to correspond to bathymetric features in the region (Maharaj et al. 2004)

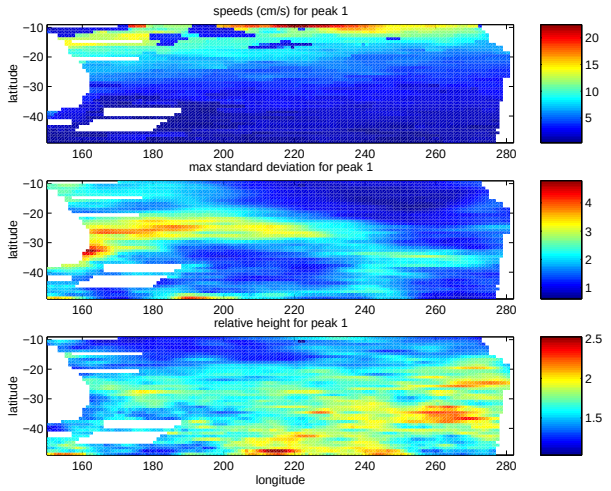

Figure 1: speeds (cm/s), standard deviation of energy (arbitrary units) and relative height for peak 1 in RT analysis

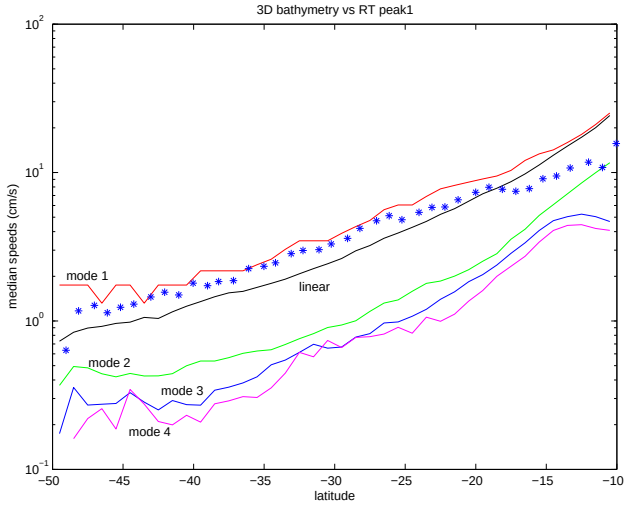

Figure 2: comparison of peak 1 median speeds to linear estimates and modes 1 to 4 of a high resolution bathymetry model run

The greatest energetic variability is in the western side of the basin—in a band between 20°S and 30°S in the western Pacific, the EAC return flow and south of New Zealand. There is significant energy in a small zonal band between 30°S and 40°S which spreads meridionally around 240°E to 250°E (in the region of the East Pacific Rise and the Pacific Antarctic Rise) then two separate zonal bands between 20°S and 30°S and south of 40°S with very low variability in between. There is some suggestion here of a relationship to bathymetry (Maharaj et al. 2004).

The greatest relative heights, that is, the most significant peaks, are in the south east of the basin with values ranging from 1.8 to 2.5. The patterns here are also suggestive of bathymetric interaction. For example, some peaks coincide with ridges in the south east. Lowest relative heights are in the north west of the basin where the peaks are not significantly different from the mean value.

Figure 2 is a comparison of the median speed at each latitude to the first baroclinic Rossby wave speed estimates based on linear theory and the first to fourth order baroclinic Rossby waves from the modified theory of Killworth and Blundell (2003a,b). It shows that southward of 20°S, median speeds from the 2D-RT analysis lie between first mode estimates from the two theories. Equatorward of 20°S, speeds are significantly lower but are still much faster than the higher order modes save for one estimate at 11°S which coincides with mode 2. These slow median speed estimates are largely due to the anomalously slow speeds seen in the north western part of the basin and have been examined in some detail by Maharaj et al., (2004).

Figure 3 displays the equivalent information provided in Figure 1 for the second peak in the 2D-RT analysis. Missing values denote that no second peak was present. Peak 2 speeds are almost everywhere consistently low (O $<$ 2 cm/s) with the exception of two regions. Around 40°S, 200°E-220°E, there are some speeds of around 10cm/s. The second region is that pointed out in peak 1

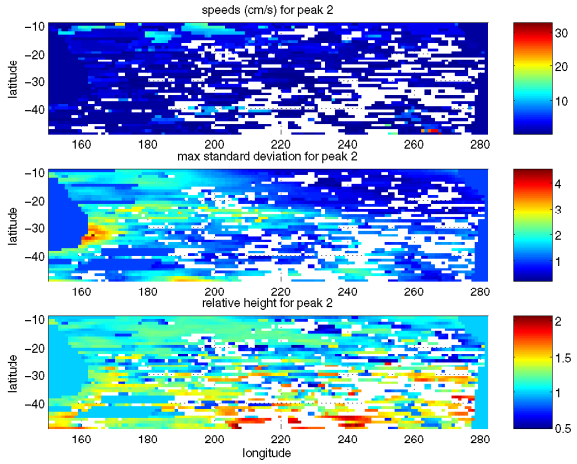

Figure 3: speeds (cm/s), standard deviation of energy (arbitrary units) and relative height for peak 2 in RT analysis

for anomalously low speeds (around 10°S 150-170°E and 180-210°E). In peak 2, these regions show higher speeds of approximately 10-12 cm/s.

As in peak 1, maximum standard deviation shows that the greatest energetic variability in peak 2 is also in the western Pacific. Maximum values also lie in similar spatial locations as peak 1. Relative height values in the western half of the basin are comparable to the relative heights of peak 1 in the same location. This would indicate that the second peak here is important. The most significant relative heights are, again, in the south east of the basin.

Latitudinal median speeds for peak 2 (Figure 4) show consistently low speeds over the entire basin. Speeds between 10°S and 20°S fall around 4cm/s and gradually fall till 30°S where values show no real pattern. The second peak in the RT shows median speeds increasing polewards From 10°S to 30°S, peak 2 speeds fall around or slightly

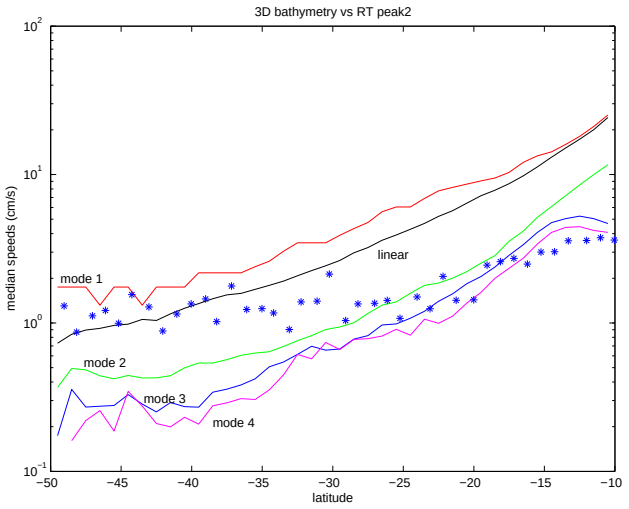

Figure 4: comparison of peak 2 median speeds to linear estimates and modes 1 to 4 of a high resolution bathymetry model run

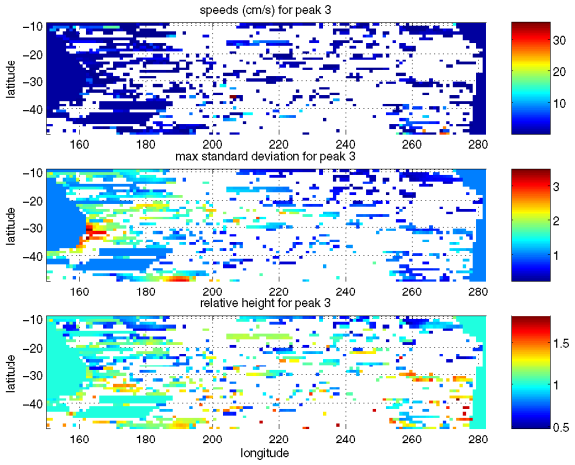

Figure 5: speeds (cm/s), standard deviation of energy (arbitrary units) and relative height for peak 3 in RT analysis

below mode 2-4 estimates. From 30°S to 35°S, they fall between linear and mode 2 estimates. Polewards of 35°S, estimates are largely between linear mode 1 and perturbed mode 1 estimates.

Figure 5 are the results for the third peak in the 2D-RT analysis. Note that there are now even fewer pixels with values indicating that no third peak was present for most of the basin.

Speeds are mostly very slow with some anomalously high speeds scattered all over the basin. These speeds range around 10cm/s and a few isolated points at over 25cm/s. A comparison by eye of these pixels indicates that they have very low relative height ratios and hence are most likely spurious.

Maximum standard deviation shows that variability is similar to the first two peaks. Highest values are in the EAC

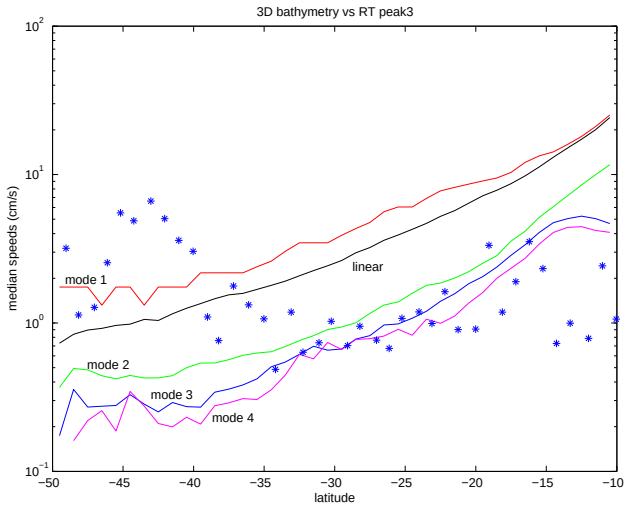

Figure 6: comparison of peak 3 median speeds to linear estimates and modes 1 to 4 of a high resolution bathymetry model run

return flow and south east of New Zealand. Highest relative height values for peak 3 are again in the south east but the number of points here are low. The largest presence of peak 3 occurs in the mid and western basin. These show relative heights of between 1 and 1.5 so are likely to be real.

A comparison of median speeds (Figure 6) indicates very slow speeds between 20°S and 35°S with speeds increasing equatorwards and polewards. Between 25°S and 35°S, most speed estimates are close to or around modes 2 to 4. Equatorwards of 25°S, speeds are largely below mode 4. From 35°S to 40°S, speeds are between linear and mode 2 and polewards of 40°S, speeds are faster than mode 1. Note, however, that there are a very small number of samples with a third peak and while peaks are being screened through the calculation of relative heights, no peaks have been discarded. Peaks with relative heights below 1 should be cast aside as quality control.

4.2 2D Fourier Transform

Figure 7 shows the speeds computed from the first peak in the 2D-FT analysis and its amplitude. There are very fast speeds (20 cm/s) around New Zealand and small regions east and west of the basin around 10°S. North of 20°S are fairly slow speeds of greater than 7cm/s and in particular between 190°E and 220°E. This is also apparent in the RT analysis. These values are significantly below the first mode linear or perturbed estimates. Polewards of 20°S, with the exception of around New Zealand, speeds are slow (less than 5cm/s) but fall within linear and perturbed estimates (Figure 8)

The maximum energetic signature is very similar to that produced by the 2D-RT analysis. The most energetic part of the region is a zonal band between 20°S and 35°S, west of

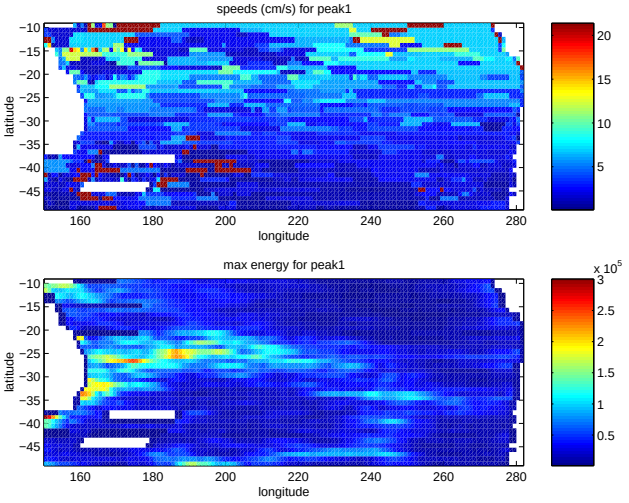

Figure 7: speeds and energy for peak 1 from the FT analysis

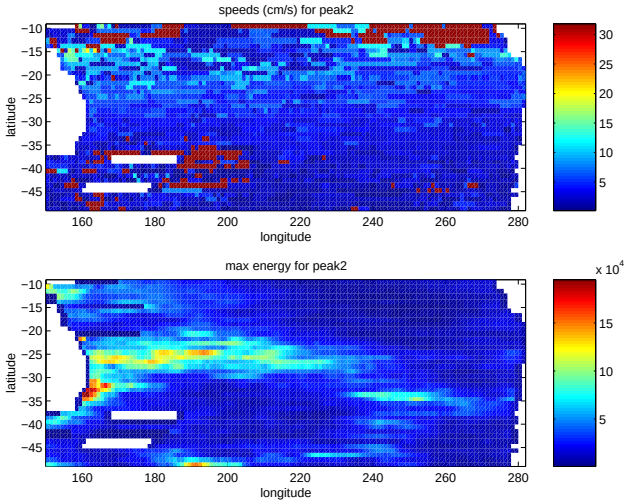

Figure 9: speeds and energy for peak 2 from the FT analysis

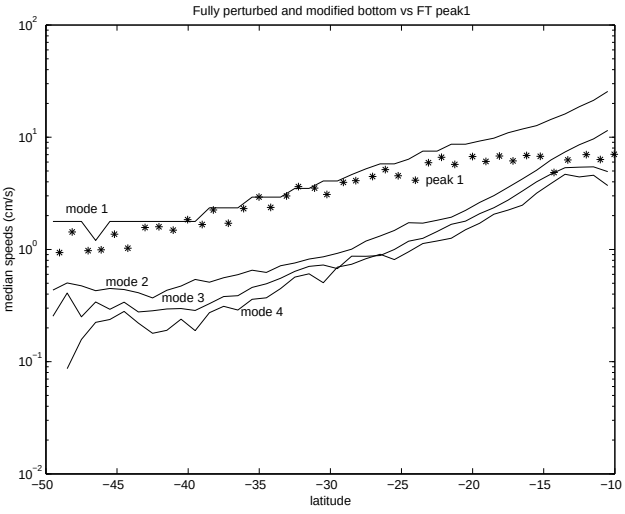

Figure 8: comparison of peak 1 median speeds to modes 1 to 4 of a fully perturbed model run

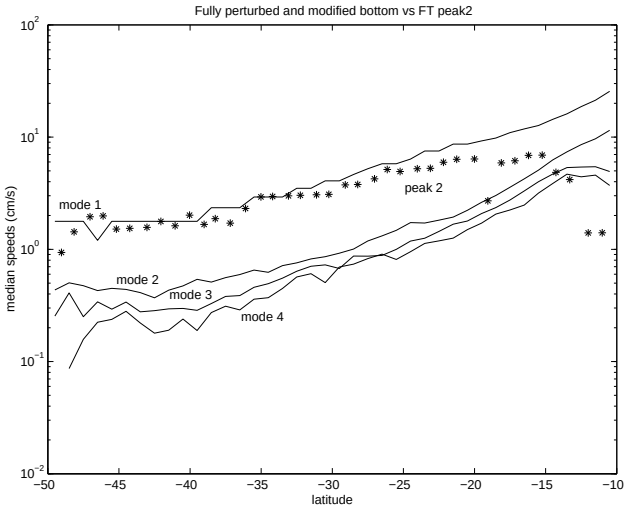

Figure 10: comparison of peak 2 median speeds to modes 1 to 4 of a fully perturbed model run

around 220°E in the region of the EAC. There is some high variability south of 30°S and 240°E, a peak around 190°E, 45°S (south east of New Zealand) and between 10°S to 15°S, west of 175°E.

The speeds and peak amplitude for peak 2 are shown in Figure 9 and median speed comparisons in Figure 10. A large area of the tropics show faster speeds here than in peak 1, especially in the eastern tropics. Again, very fast speeds are seen around New Zealand. Comparison to linear and perturbed modes indicates speeds close to perturbed first mode values. Peak amplitude is similar to peak 1 energy. Figures 11 and 12 show similar values for peak 3.

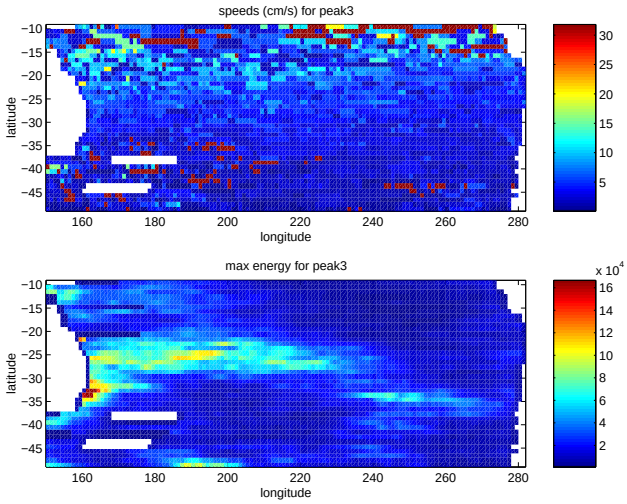

Figure 11: speeds and energy for peak 3 from the FT analysis

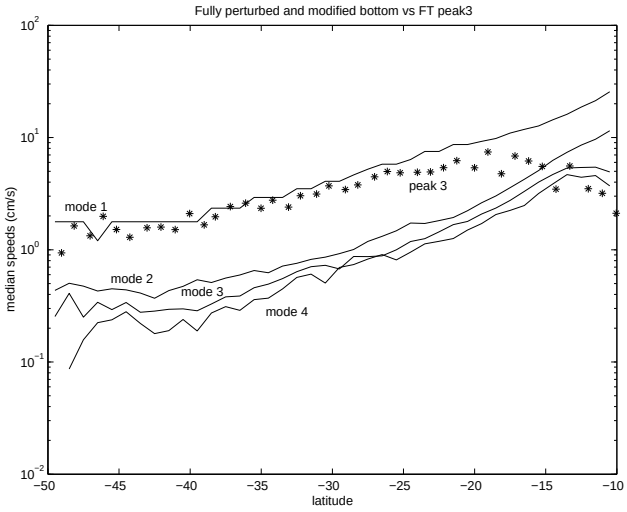

Figure 12: comparison of peak 3 median speeds to modes 1 to 4 of a fully perturbed model run

5 Discussion and Conclusion

This study tested the hypothesis that multiple peaks in the Radon and Fourier Transform analysis of sea level anomalies may correspond to higher order Rossby wave baroclinic modes over the entire South Pacific Ocean basin. The first three peaks of the Radon and Fourier Transform were found and described in terms of peak amplitude and estimated speeds. For the Radon Transform, relative heights were calculated as a means to screen peaks. Estimated speeds were then compared against speeds for the first baroclinic Rossby wave mode based on linear theory as well as speeds for the first four baroclinic modes for a fully modified and perturbed ocean with high resolution bathymetry (Killworth and Blundell 2003a,b), commonly referred to as the ”perturbed” or ”modified” theory.

For the Radon Transform analysis, speeds calculated from the first peak generally fell between estimates for the first baroclinic mode propagation speed from linear and the modified theory. Results from the higher order modes, however, were more equivocal. The relationship between secondary peaks and the higher order speed estimates varied with latitude. While the second and third peaks yielded speeds that fell within the range of higher order baroclinic modes in the lower to mid latitudes (between 15°S and 30°S) , they were significantly faster in the high latitudes. It is important to note that while relative heights were calculated, no peaks were excluded in these results. As a first measure, relative heights below a threshold of 1 must be removed to quality control the peaks before any physical meaning is given to the results. It is also interesting to note that the second and third peaks are not ubiquitous over the basin. On the contrary, higher order peaks are successively harder to find. This result supports the general idea that no more than the first three modes are important for Rossby wave propagation.

The energetic variability and speed estimates for the first peak in the Fourier Transform results generally agree well with the Radon Transform results, i.e, very slow speeds equatorwards of 20°S but otherwise between linear and modified estimates for the first baroclinic Rossby wave. The second and third peaks, however, show little resemblance to second and third peaks in the Radon Transform. In fact, apart from slower speed estimates equatorwards of 20°S, the rest of the speed estimates resemble the first peak estimates. Clearly, we are not capturing the higher order peaks, if they exist and are resolved in the Fourier analysis. The secondary peaks being captured in the analysis is more likely leakage from the first peak. A more rigorous method for scanning for secondary peaks needs to be established to first of all, confirm whether these spectral peaks exist. If so, then a method for screening peaks is also warranted.

These results illustrate what may be inherent differences between the Radon and Fourier Transform analysis. While the Radon Transform seems to easily capture multiple ”modes” of signal in the longitude-time or Hovmöller plots, the Fourier Transform seems to largely focus on the most dominant signal. The Fourier Transform may also be more heavily dependent on the length and resolution of the

dataset. Therefore it may be more appropriate to vary the window length of the analysis over different latitudes.

Acknowledgments The altimeter products were produced by the CLS Space Oceanography Division as part of the Environment and Climate EU ENACT project (EVK2-CT2001-00117) and with support from CNES. The authors would like to thank Peter Killworth and Jeff Blundell for providing the perturbed speed estimates. A large portion of this work was carried out during A. Maharaj's visit to Southampton Oceanography Centre, UK. A. Maharaj is supported by an Australian Postgraduate Award.

References

Challenor, P. G., P. Cipollini and D. Cromwell, 2001: Use of the 3D Radon Transform to examine the properties of oceanic Rossby waves, *J. Atmos. Oceanic Technol.*, **18**, 1558–1566.

Cipollini, P., D. Cromwell, P. G. Challenor and S. Raffaglio, 2001: Rossby waves detected in global ocean colour data, *Geophys. Res. Lett.*, **28**(2), 323–326.

———, ———, M. S. Jones, G. D. Quartly and P. G. Chellenor, 1997: Concurrent altimeter and infrared observations of rossby wave propagation near 34°N in the Northeast Atlantic, *Geophys. Res. Lett.*, **24**, 885–892.

———, G. D. Quartly, P. G. Challenor, D. Cromwell and I. S. Robinson, 2004: *Manual of Remote Sensing*, chapter Remote sensing of extra-equatorial planetary waves in the oceans.

Deans, S. R., 1983: *The Radon transform and some of its applications*, John Wiley.

Fu, L. L., and D. B. Chelton, 2001: *Satellite Alitmetry and Earth Sciences*, chapter Large scale ocean circulation, pp. 133–169, Academic Press.

Gill, A. E., 1982: *Atmosphere-ocean dynamics*, Academic Press, Inc, 662pp.

Hill, K. L., I. S. Robinson and P. Cipollini, 2000: Propagation characteristics of extratropical planetary waves observed in the atsr global sea surface temperature record, *J. Geophys. Res.*, **105**, 21927–21945.

Killworth, P. D., and J. R. Blundell, 2003a: Long extra-tropical planetary wave propagation in the presence of slowly varying mean flow and bottom topography. I: the local problem, *J. Phys. Oceanogr.*, **33**, 784–801.

———, and ———, 2003b: Long extra-tropical planetary wave propagation in the presence of slowly varying mean flow and bottom topography. II: ray propagation and comparison with observations, *J. Phys. Oceanogr.*, **33**, 802–821.

Maharaj, A., P. Cipollini and N. Holbrook, 2004: The influence of bottom topography on long Rossby wave propagation in the South Pacific Ocean, *Geophys. Res. Lett.*, (submitted).

Subrahmanyam, B., I. S. Robinson, J. R. Blundell and P. G. Challenor, 2001: Rossby waves in the indian ocean from TOPEX/POSEIDON altimeter and model simulations, *Int. J. Remote Sensing*, (in press).

Traon, P. Y. L., P. Gaspar, F. Bouyssel and H. Makhmara, 1995: Using topex/poseidon data to enhance ers-1 data, *J. Atmos. Oceanic Technol.*, **12**, 161–170.

———, and F. Ogor, 1998: Ers-1/2 orbit improvement using topex/poseidon: the 2 cm challenge, *J. Geophys. Res.*, **103**, 8045–8057.